Gauge dependence of atomic inner-shell transition rates from Dirac-Fock wave functions

Mau Hsiung Chen
Department of Physics and Chemical Physics Institute, University of Oregon, Eugene, Oregon 97403

Bernd Crasemann*
Stanford Synchrotron Radiation Laboratory and Department of Physics, Stanford University, Stanford, California 94305
(Received 7 March 1983)

Relativistic radiative and radiationless atomic inner-shell transition rates have been calculated with Dirac-Fock wave functions with the use of matrix elements that correspond to different gauges. Radiative rates computed in the length gauge are found to be larger than Coulomb-gauge results; for K-shell radiative widths, the difference is $\sim 20\%$ at $Z=10$ and falls to $\sim 4\%$ at $Z=30$; the difference for L_2 radiative widths is a factor of 2 at $Z=18$ and $\sim 7\%$ at $Z=48$. Especially large discrepancies between length- and Coulomb-gauge results are found for $\Delta n=0$ radiative transition rates. Auger transition rates calculated in the Lorentz and Coulomb gauges agree to better than 1% in all cases tested here; it is inferred that in first-order perturbation theory the Auger rate is practically gauge invariant. Certain general features of the effects of relativity on radiationless transitions are also discussed. These effects can arise from relativistic changes in the transition energies, relativistic orbital effects, and relativistic aspects of the pertinent operators. The relative importance of these factors is evaluated.

I. INTRODUCTION

The role of gauge invariance in the interaction between the electromagnetic field and the electron-positron field is discussed explicitly in well-known texts.[1,2] The expressions for transition matrix elements depend on the choice of gauge. Certainly, the numerical results should be gauge invariant if exact wave functions were used. But exact atomic wave functions are not known, and the most efficient relativistic atomic model which is suitable for treating inner-shell transitions is based on the relativistic self-consistent-field method. In the approximate calculations of relativistic radiative transition rates from Dirac-Fock wave functions, the numerical results become gauge dependent because of the nonlocal potential introduced in the Dirac-Fock effective Hamiltonian.[3] All existing relativistic self-consistent-field calculations of radiative atomic transition probabilities have, however, been carried out in the Coulomb or length gauge.[4–7] No attempt appears to have been made heretofore to compare Dirac-Fock results obtained in different gauges.

In the nonrelativistic theory, radiative electric dipole transitions can be expressed in terms of a dipole-length, dipole-velocity, or dipole-acceleration matrix element. These expressions are equivalent in a single-particle model, but they lead to different numerical results, for example, in a Hartree-Fock approach.[3,8] The length and velocity forms constitute the nonrelativistic limits of relativistic expressions in different gauges (Sec. II A).

For radiationless (Auger and Coster-Kronig) transitions, all relativistic calculations performed to date[9–15] are based on Møller's two-electron operator, which is in the Lorentz gauge. The question of gauge dependence of relativistic radiationless transitions computed with approximate wave functions has never been explored.

In order to investigate the extent of gauge dependence in Dirac-Fock calculations of atomic inner-shell transitions, we have performed a set of exploratory computations. We have calculated relativistic radiative transition rates to K- and L-shell vacancy states, using Dirac-Fock wave functions and employing both the Coulomb gauge and the length gauge. The differences between these two sets of results can shed some light on the uncertainty of independent-particle Dirac-Fock calculations. We have also performed relativistic computations of radiationless rates with Dirac-Fock wave functions, using both the Lorentz gauge and the Coulomb gauge. Results were calculated for K and L shells of selected elements in various different ranges of atomic numbers.

We also discuss certain general features of the effects of relativity on radiationless transitions. These effects can arise from several different factors: (i) relativistic changes in transition energies; (ii) relativistic orbital effect caused by the inclusion of the mass-velocity correction, the Darwin term, and spin-orbit interaction in the Dirac equations; and (iii) relativistic aspects of the pertinent operators, viz., the magnetic interaction and retardation correction in the two-electron operator, due to electron-photon coupling. The relative importance of these factors is evaluated.

II. RELATIVISTIC THEORY

A. Radiative transitions

In the theory of quantum electrodynamics, the interaction potential between the electromagnetic field and the electron-positron field depends on the choice of gauge.[1,2] The expression for the electric multipole transition matrix, in turn, also becomes gauge dependent. The spontaneous emission rate for a transition $i \rightarrow f$, in atomic units, is[16]

$$A_{i\to f}=2\omega\sum_L\frac{(2j_f+1)}{(2L+1)}\begin{pmatrix} j_i & L & j_f \\ \frac{1}{2} & 0 & -\frac{1}{2}\end{pmatrix}^2(|M_{fi}^{(e)}(g_L)|^2+|\bar{M}_{fi}^{(m)}|^2)\,, \tag{1}$$

where

$$\bar{M}_{fi}^{(e)}(g_L)=\bar{M}_{fi}^{(e)}(0)+g_L\bar{M}_{fi}^{(l)}\,, \tag{2}$$

$$\bar{M}_{fi}^{(e)}(0)=i^L\left[\left[\frac{L}{L+1}\right]^{1/2}[(\kappa_f-\kappa_i)I_{L+1}^{+}+(L+1)I_{L+1}^{-}]-\left[\frac{L+1}{L}\right]^{1/2}[(\kappa_f-\kappa_i)I_{L-1}^{+}-LI_{L-1}^{-}]\right]\,, \tag{3}$$

$$\bar{M}_{fi}^{l}=i^L[(2L+1)J^{(L)}+(\kappa_f-\kappa_i)(I_{L+1}^{+}+I_{L-1}^{+})-LI_{L-1}^{-}+(L+1)I_{L+1}^{-}]\,, \tag{4}$$

and

$$\bar{M}_{fi}^{m}=i^{L+1}\frac{2L+1}{[L(L+1)]^{1/2}}(\kappa_f+\kappa_i)I_L^{+}(\omega)\,. \tag{5}$$

The $I_L^{\pm}(\omega)$ and $J^{(L)}(\omega)$ integrals are defined as follows[4,16]:

$$I_L^{\pm}(\omega)=\int_0^{\infty}(G_fF_i\pm F_fG_i)j_L(\omega r)dr\,, \tag{6}$$

$$J^{(L)}(\omega)=\int_0^{\infty}(G_fG_i+F_fF_i)j_L(\omega r)dr\,. \tag{7}$$

Here, ω is the photon wave number $(E_i-E_f)/c$; j_i, κ_i, and E_i are, respectively, the total angular momentum, relativistic quantum number, and energy of the initial state. The corresponding quantities for the final state are j_f, κ_f, and E_f. The relativistic radial wave function has G as the major and F as the minor component.

The Coulomb gauge and the length gauge correspond to the choices $g_L=0$ and $g_L=[(L+1)/L]^{1/2}$, respectively.[16] The necessary and sufficient condition for the transition matrices for all multipoles to be gauge invariant is that the transition matrix of electric multipoles for longitudinal photons vanish identically. This condition is automatically satisfied if exact wave functions are used, or for a single-particle atomic model, but it may not necessarily hold for a Dirac-Fock model.[16] For electric dipole transitions it has been shown that the Coulomb gauge leads to the dipole-velocity form in the nonrelativistic limit, while the length gauge leads to the dipole-length form.[16]

B. Radiationless transitions

The Auger transitions are treated as two-step processes. The radiationless decay probabilities are calculated from perturbation theory in the frozen-orbital approximation. The total radiationless transition probability for a transition $n_1',\kappa_1'\to n_1,\kappa_1,n_2,\kappa_2$, in j-j coupling, is[13]

$$T=\tau\frac{1}{2j_1'+1}\sum_{\substack{J,J',\\ M,M'}}\sum_{\kappa_2'}|D-E|^2\,, \tag{8}$$

where

$$D=\langle j_1'(1)j_2'(2)J'M'\,|\,V_{12}\,|\,j_1(1)j_2(2)JM\rangle\,, \tag{9}$$

$$E=\langle j_1'(1)j_2'(2)J'M'\,|\,V_{12}\,|\,j_1(2)j_2(1)JM\rangle\,, \tag{10}$$

and

$$\tau=\begin{cases}\frac{1}{2} & \text{if } n_1,\kappa_1=n_2,\kappa_2\\ 1 & \text{otherwise}\,.\end{cases} \tag{11}$$

The initial hole is characterized by the quantum numbers n_1',κ_1',j_1'; the continuum electron by n_2',κ_2',j_2', and the final holes by n_1,κ_1,j_1 and n_2,κ_2,j_2. In Eqs. (9) and (10), $|j_1(1)j_2(2)JM\rangle$ denotes the (not antisymmetrized) j-j–coupled two-hole wave function. The continuum wave function is assumed to be normalized so as to represent one electron ejected per unit time.[9] Atomic units are used throughout.

In the nonrelativistic theory, the two-electron operator represents just the Coulomb repulsion between the two electrons. In the relativistic theory, the photon-electron coupling is automatically included in the two-electron operator. From quantum electrodynamics, the electron-electron interaction operator is gauge dependent.

In the currently available relativistic Auger calculations,[9–15] the two-electron operator is chosen to be the Møller operator, which is based on the Lorentz gauge:

$$V_{12}^{M}=(1-\vec{\alpha}_1\cdot\vec{\alpha}_2)e^{i\omega r_{12}}/r_{12}\,. \tag{12}$$

In the Coulomb gauge, the two-electron operator is[17]

$$V_{12}^{C}=\frac{1}{r_{12}}-(\vec{\alpha}_1\cdot\vec{\alpha}_2)\frac{e^{i\omega r_{12}}}{r_{12}}+(\vec{\alpha}_1\cdot\vec{\nabla}_1)(\vec{\alpha}_2\cdot\vec{\nabla}_2)\frac{e^{i\omega r_{12}}-1}{\omega^2 r_{12}}\,. \tag{13}$$

Here, the $\vec{\alpha}_i$ are Dirac matrices, and ω is the wave number of the virtual photon.

In relativistic theory, the Auger matrix elements are calculated in j-j coupling and can be separated into angular and radial parts with the aid of Racah algebra. For the Møller operator, a detailed derivation can be found in Ref. 13. The relativistic matrix element in the Coulomb gauge [Eq. (13)] has been reduced in Ref. 17 to a form that is suitable for easy numerical computation.

The direct matrix element of the two-electron operator in the Coulomb gauge is[17]

$$D=\sum_{\lambda=0}^{\infty}A_\lambda\left\{\left[\langle W_{11}\gamma_\lambda^C W_{22}\rangle+\left[\frac{\lambda}{2\lambda-1}\langle P_{11}^\lambda\gamma_{\lambda-1}P_{22}^\lambda\rangle+\frac{\lambda+1}{2\lambda+3}\langle Q_{11}^\lambda\gamma_{\lambda+1}Q_{22}^\lambda\rangle\right]\right]\Pi(l_1',\lambda,l_1)\Pi(l_2',\lambda,l_2)\right.$$
$$-(1-\delta_{\lambda0})\frac{(\kappa_1'+\kappa_1)(\kappa_2'+\kappa_2)}{\lambda(\lambda+1)}\langle U_{11}\gamma_\lambda U_{22}\rangle\Pi(l_1',\lambda+1,l_1)\Pi(l_2',\lambda+1,l_2)$$
$$+\left[-\frac{\lambda}{2\lambda-1}\langle V_{11}\gamma_{\lambda-1}P_{22}\rangle+\frac{\lambda+1}{2\lambda+3}\langle V_{11}\gamma_{\lambda+1}Q_{22}\rangle+\lambda(\lambda+1)(\langle P_{11}S_\lambda Q_{22}\rangle+\langle Q_{11}t_\lambda P_{22}\rangle)\right]$$
$$\left.\times\Pi(l_1',\lambda,l_1)\Pi(l_2',\lambda,l_2)\right\}, \tag{14}$$

where

$$A_\lambda=(-1)^{j_2+j_2'+J}[(2j_1+1)(2j_2+1)(2j_1'+1)(2j_2'+1)]^{1/2}\begin{Bmatrix}j_1' & j_2' & J\\ j_2 & j_1 & \lambda\end{Bmatrix}\begin{pmatrix}j_1' & j_1 & \lambda\\ -\frac{1}{2} & \frac{1}{2} & 0\end{pmatrix}\begin{pmatrix}j_2' & j_2 & \lambda\\ -\frac{1}{2} & \frac{1}{2} & 0\end{pmatrix}, \tag{15}$$

$$P_{ij}^\lambda(r)=[(\kappa_j-\kappa_i')/\lambda]U_{ij}(r)+V_{ij}(r)\,, \tag{16}$$

$$Q_{ij}^\lambda(r)=[(\kappa_j-\kappa_i')/(\lambda+1)]U_{ij}(r)-V_{ij}(r)\,, \tag{17}$$

$$W_{ij}(r)=G_i'(r)G_j(r)+F_i'(r)F_j(r)\,, \tag{18}$$

$$U_{ij}(r)=G_i'(r)F_j(r)+F_i'(r)G_j(r)\,, \tag{19}$$

$$V_{ij}(r)=G_i'(r)F_j(r)-F_i'(r)G_j(r)\,, \tag{20}$$

$$\gamma_\lambda^C(r_1,r_2)=r_<^\lambda/r_>^{\lambda+1}\,, \tag{21}$$

$$\gamma_\lambda(r_1,r_2)=-(2\lambda+1)\omega j_\lambda(\omega r_<)\mathscr{Y}_\lambda(\omega r_>)+i(2\lambda+1)\omega j_\lambda(\omega r_<)j_\lambda(\omega r_>)\,, \tag{22}$$

$$S_\lambda=\begin{cases}\dfrac{1}{r_1}j_{\lambda+1}(\omega r_2)\mathscr{Y}_\lambda(\omega r_1)-\dfrac{i}{r_1}j_{\lambda+1}(\omega r_2)j_\lambda(\omega r_1), & r_1\ge r_2\\ \dfrac{r_1^{\lambda-1}}{\omega^2 r_2^{\lambda+2}}+\dfrac{1}{r_1}j_\lambda(\omega r_1)\mathscr{Y}_{\lambda+1}(\omega r_2)-\dfrac{i}{r_1}j_\lambda(\omega r_1)j_{\lambda+1}(\omega r_2), & r_1<r_2\end{cases} \tag{23}$$

$$t_\lambda=\begin{cases}\dfrac{r_2^{\lambda-1}}{\omega^2 r_1^{\lambda+2}}+\dfrac{1}{r_1}j_{\lambda-1}(\omega r_2)\mathscr{Y}_\lambda(\omega r_1)-\dfrac{i}{r_1}j_{\lambda-1}(\omega r_2)j_\lambda(\omega r_1), & r_1\ge r_2\\ \dfrac{1}{r_1}j_\lambda(\omega r_1)\mathscr{Y}_{\lambda-1}(\omega r_2)-\dfrac{i}{r_1}j_\lambda(\omega r_1)j_{\lambda-1}(\omega r_2), & r_1<r_2\end{cases} \tag{24}$$

$$\langle W_{11}\gamma_\lambda^C W_{22}\rangle=\int_0^\infty\int_0^\infty W_{11}(r_1)\gamma_\lambda^C(r_1,r_2)W_{22}(r_2)dr_1dr_2\,, \tag{25}$$

and

$$\Pi(l',\lambda,l)=\begin{cases}1 & \text{if } l'+\lambda+l \text{ is even}\,,\\ 0 & \text{otherwise}\,.\end{cases} \tag{26}$$

The quantity $r_<$ ($r_>$) is the smaller (larger) of r_1 and r_2, and j_λ and $\mathscr{Y}_\lambda$ are spherical Bessel functions of the first and second kind, respectively.

The exchange matrix elements can be obtained by performing the exchange operation $n_1,\kappa_1\leftrightarrow n_2,\kappa_2$ on the direct matrix elements [Eq. (14)] and multiplying by the phase factor $(-1)^{J-j_1-j_2}$.

The direct matrix element of the Møller operator can be found from Eq. (14) by dropping the last bracket and changing $\langle W_{11}\gamma_\lambda^C W_{22}\rangle$ into $\langle W_{11}\gamma_\lambda W_{22}\rangle$.

The two-electron matrix elements of V_{12}^M and V_{12}^C are identical whenever the unperturbed electron orbitals satisfy Dirac equations in a local potential.[18] The relativistic Auger rate is therefore gauge invariant in the Dirac-Hartree-Slater model. The matrix elements of V_{12}^M and V_{12}^C are not necessarily identical when they are evaluated with Dirac-Fock electron orbitals. In the nonrelativistic limit Eqs. (12) and (13) lead to different expressions. It is known, however, that the on-shell matrix elements of Eqs. (12) and (13) give the same results.[19] Brown and Ravenhall[20] make a convincing physical argument that the Coulomb gauge is preferable because the dominant interaction, which is the Coulomb interaction, is in essence treated exactly in this gauge. There exists no proof, however, that this is the optimum choice.

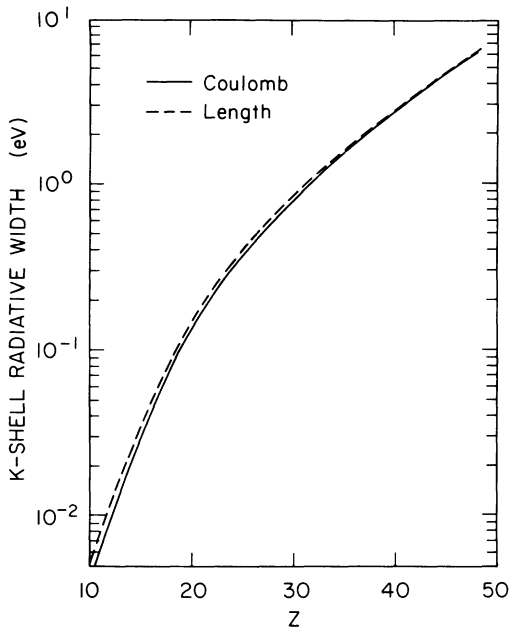

FIG. 1. Radiative widths (in eV) of atomic [1s] hole states, as functions of atomic number Z. Solid curve represents results computed in the Coulomb gauge; the dashed curve indicates results obtained in the length gauge. Dirac-Fock wave functions were used throughout.

III. NUMERICAL CALCULATIONS

The radiative transition rates are calculated in the frozen-orbital approximation, both in the Coulomb gauge and in the length gauge, with the use of Dirac-Fock wave functions[21] that correspond to the initial hole-state configurations. The transition energies are calculated from relativistic binding energies that include relaxation and quantum-electrodynamic corrections.[22]

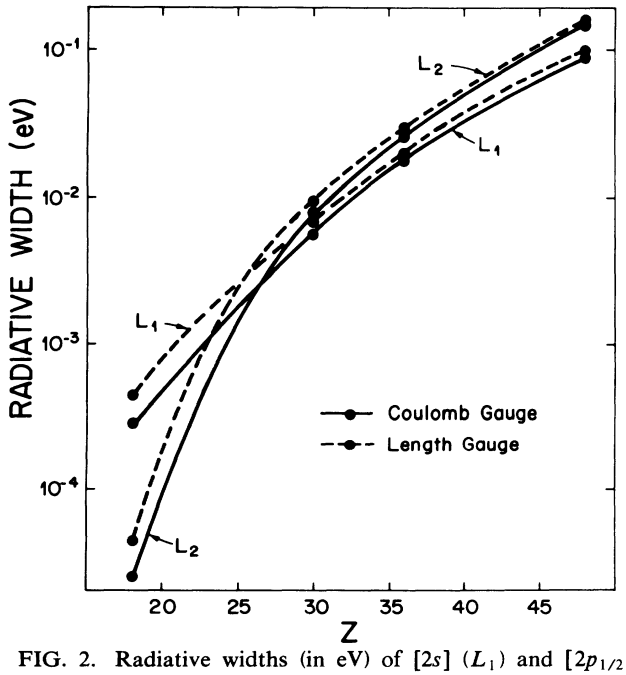

FIG. 2. Radiative widths (in eV) of [2s] (L_1) and [$2p_{1/2}$] (L_2) hole states in atoms of atomic number Z. Relativistic calculations with Dirac-Fock wave functions were performed in the Coulomb gauge (solid curves) and in the length gauge (dashed curves).

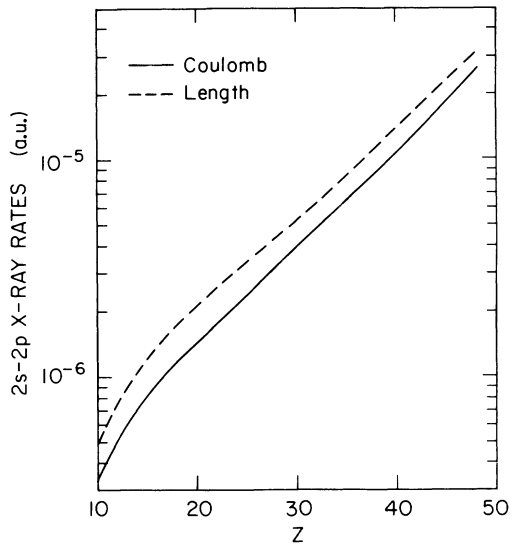

FIG. 3. Radiative 2s-2p transition probabilities (in a.u.) as functions of atomic number Z. Relativistic results in the Coulomb gauge (solid curve) are compared with rates computed in the length gauge (dashed curve).

The Auger matrix elements are computed both in the Coulomb gauge and in the Lorentz gauge, with Dirac-Fock wave functions[21] corresponding to the initial states with one inner-shell vacancy. The continuum wave functions are obtained by solving the Dirac equations in the V^{N-1} potential without the exchange contribution. The continuum wave functions are then orthogonalized to the bound-state wave functions. We use the *j-j* configuration-average energies in the calculations. These average Auger energies were found by the use of the "Z + 1 rule" with theoretical neutral-atom binding energies.[22] The continuum wave functions are normalized in the asymptotic region by matching them with asymptotic Coulomb wave functions.[9,11]

In order to explore the general characteristics of relativistic effects on Auger transitions, we have calculated Auger rates with Dirac-Hartree-Slater wave functions and several different two-electron operators: the Coulomb interaction

$$\frac{1}{r_{12}}\ , \tag{27a}$$

the Coulomb and magnetic interaction without retardation correction

$$(1-\vec{\alpha}_1\cdot\vec{\alpha}_2)\frac{1}{r_{12}}\ , \tag{27b}$$

and the retarded Coulomb and magnetic interaction

$$(1-\vec{\alpha}_1\cdot\vec{\alpha}_2)\frac{e^{i\omega r_{12}}}{r_{12}}\ . \tag{27c}$$

Results are compared with those from nonrelativistic

TABLE I. Relativistic K-LL Auger rates (in 10^{-3} a.u.), computed with Dirac-Fock wave functions in the Coulomb and Lorentz gauges.

	$Z=10$		$Z=36$		$Z=48$		$Z=80$	
Transition	Coulomb	Lorentz	Coulomb	Lorentz	Coulomb	Lorentz	Coulomb	Lorentz
K-L_1L_1	1.207	1.208	2.652	2.662	3.446	3.464	8.403	8.449
K-L_1L_2	1.132	1.133	2.937	2.948	3.974	3.989	13.155	13.182
K-L_1L_3	2.227	2.229	4.824	4.846	5.393	5.424	7.585	7.619
K-L_2L_2	0.150	0.150	0.474	0.475	0.543	0.544		0.746
K-L_2L_3	3.751	3.757	10.631	10.692	11.511	11.600		13.626
K-L_3L_3	2.157	2.160	5.774	5.803	5.950	5.991		5.921

Hartree-Slater calculations with either relativistic or nonrelativistic Auger transition energies, in order to study the relative importance of the various aspects of the effects of relativity.

IV. RESULTS AND DISCUSSION

A. Gauge dependence of Dirac-Fock results

We employed the Coulomb gauge and the length gauge in calculating radiative transition rates to K- and L-shell vacancies of selected elements with atomic numbers $10 \leq Z \leq 48$. The computations are relativistic, based on Dirac-Fock wave functions. Total rates from the present Coulomb-gauge calculations agree to better than 1% with Scofield's[6] Dirac-Fock results including relaxation.

The length gauge is generally found to yield larger radiative transition rates than the Coulomb gauge. For K-shell radiative widths, the difference is $\sim 20\%$ at $Z=10$ and falls off to $\sim 4\%$ at $Z=30$ (Fig. 1). For the L_2 radiative widths, the difference is approximately a factor of 2 at $Z=18$, falling to $\sim 7\%$ at $Z=48$ (Fig. 2). For individual transitions with $\Delta n=0$, the discrepancy between length- and Coulomb-gauge results is large and persists to moderately heavy elements, e.g., 20% for $2s$-$2p$ transitions at $Z=48$ (Fig. 3).

Auger transition rates were calculated in the Lorentz gauge and in the Coulomb gauge, for K- and L-shell initial vacancies in closed-shell atoms with atomic numbers $10 \leq Z \leq 80$. Dirac-Fock wave functions were used in these relativistic computations. Some of the results for K-LL transitions are listed in Table I. The two different gauges are found to lead to radiationless transition rates that agree to better than 1% in all cases. This is consistent with the fact that the on-shell matrix elements of Eqs. (12) and (13) give the same results. We thus conclude that in first-order perturbation theory the Auger rate is practically gauge invariant.

It is interesting to note, incidentally, that total Auger transition rates calculated with Dirac-Fock wave func-

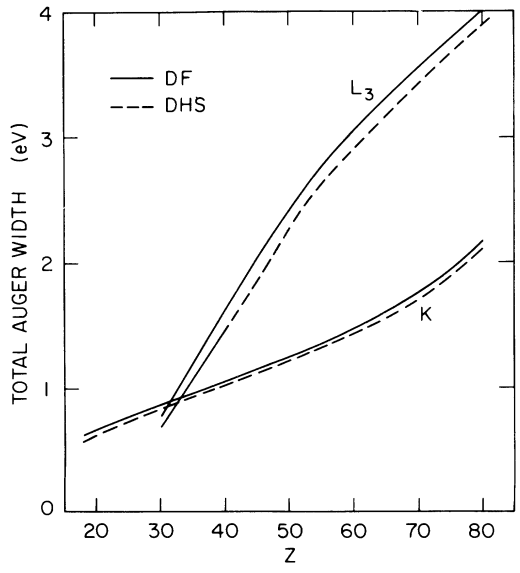

FIG. 4. Total Auger widths (in eV) of [1s] (K) and [$2p_{3/2}$] (L_3) vacancy states in atoms of atomic number Z. Solid curves were computed with Dirac-Fock wave functions; dashed curves, with Dirac-Hartree-Slater wave functions.

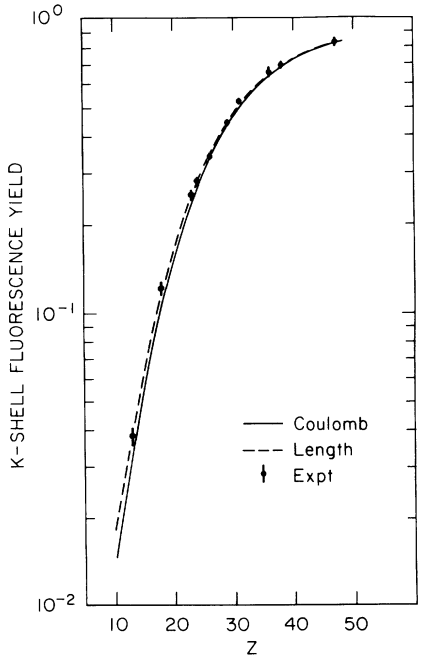

FIG. 5. Atomic K-shell fluorescence yield, as function of atomic number Z. Calculations in the Coulomb gauge (solid curve) are compared with results obtained in the length gauge (dashed curve). Experimental data are from Ref. 23.

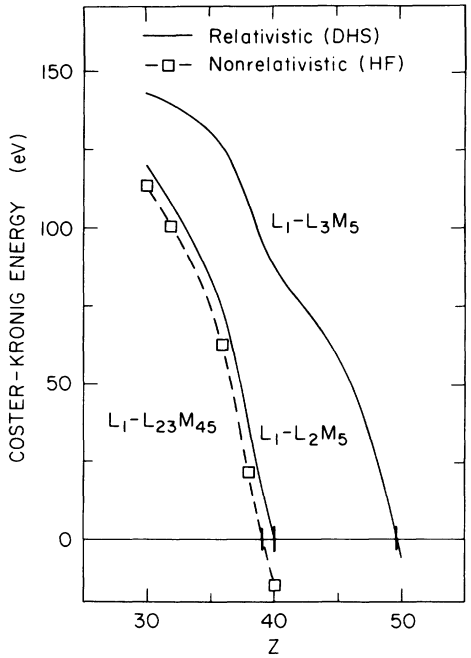

FIG. 6. Calculated L_1-$L_{2,3}M_{4,5}$ Coster-Kronig transition energies (in eV), as functions of atomic number Z. Relativistic results (solid curves) computed with Dirac-Hartree-Slater wave functions are compared with nonrelativistic energies (dashed curve) calculated with Hartree-Fock wave functions.

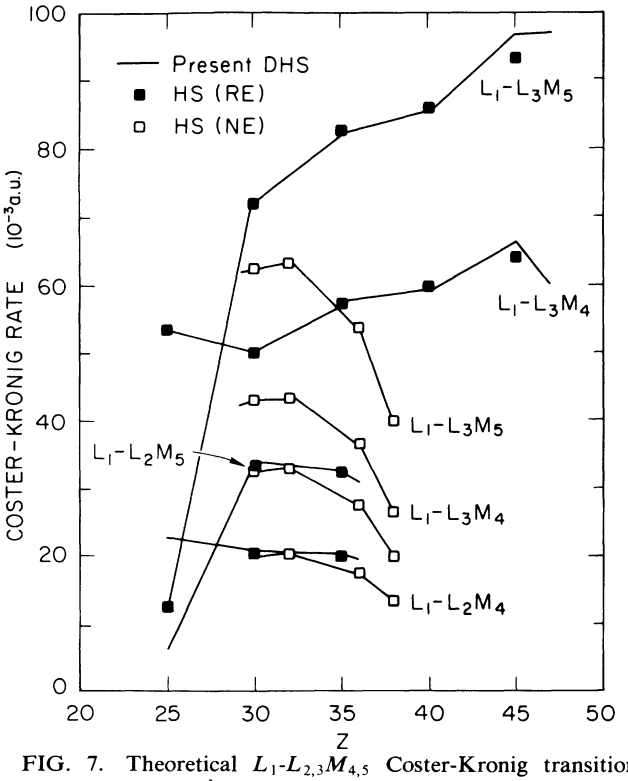

FIG. 7. Theoretical L_1-$L_{2,3}M_{4,5}$ Coster-Kronig transition probabilities (in 10^{-3} a.u.), as functions of atomic number Z. Relativistic results from Dirac-Hartree-Slater wave functions (solid curves) are compared with nonrelativistic Hartree-Slater calculations in which the same relativistic transition energies were used (solid squares) and with nonrelativistic Hartree-Slater calculations with nonrelativistic transition energies (open squares).

tions are larger than results from Dirac-Hartree-Slater wave functions; the difference for K shells falls from $\sim 10\%$ at $Z=18$ to $\sim 3\%$ at $Z=80$, and for L_3 shells, from $\sim 14\%$ at $Z=30$ to 3% at $Z=80$ (Fig. 4). The reason for these discrepancies appears to be that inclusion of the full exchange potential in the Dirac-Fock equations tends to pull the wave functions in toward the origin, thus increasing the wave-function overlap and producing a larger transition rate. A similar finding has been reported for x-ray emission rates.[6]

K-shell fluorescence yields from the present Dirac-Fock calculations with different choices of gauge are compared in Fig. 5. For $Z \gtrsim 30$, the K fluorescence yields from the Coulomb and length gauges are virtually the same, and agree very well with experiment.[23] For low-Z atoms, K fluorescence yields calculated in the length gauge seem to agree better with experiment[23] (Fig. 5).

B. Effects of relativity on radiationless transitions

Comparison of relativistic individual Auger rates with nonrelativistic results seems highly confusing at first glance; the relativistic effects are exceedingly uneven. For example, the K-L_1L_1 rates are greatly enhanced by rela-

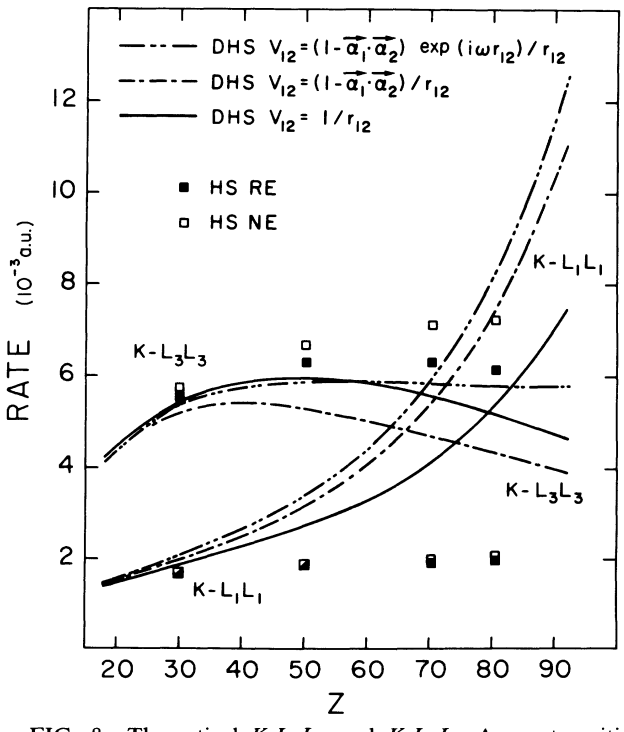

FIG. 8. Theoretical K-L_1L_1 and K-L_3L_3 Auger transition rates (in 10^{-3} a.u.) as functions of atomic number Z. Relativistic calculations with Dirac-Hartree-Slater wave functions were performed with the two-electron operators of Eq. (27c) (—··—), Eq. (27b) (— · —), and Eq. (27a) (——). Also shown are nonrelativistic results computed from Hartree-Slater wave functions with relativistic transition energies (solid squares) and with nonrelativistic transition energies (open squares).

tivity, the K-L_3L_3 rates are somewhat reduced, and K-L_2L_3 transitions are affected hardly at all.

In order to explain this apparent unevenness of the effects of relativity, we consider the different sources of relativistic effects: (i) changes in transition energy, (ii) differences between relativistic and nonrelativistic wave functions, (iii) the contribution from the current-current (magnetic) interaction, and (iv) retardation of the Coulomb and magnetic interactions. By artificially including these factors one at a time in the calculations, we can study each effect separately.

Energy effects are obviously very important for Coster-Kronig and super-Coster-Kronig rates, which generally involve low transition energies and matrix elements that are exceedingly energy sensitive (especially near threshold). In fact, without relativity, all L_2-L_3X and M_2-M_3X Coster-Kronig transitions would be energetically impossible. In Fig. 6 we compare relativistic L_1-$L_{2,3}M_{4,5}$ Coster-Kronig energies from Dirac-Hartree-Slater calculations[24] with nonrelativistic Hartree-Fock results. The relativistic L_1-L_3M_5 transition energies are seen to be roughly twice as large as the nonrelativistic energies. The Hartree-Fock results predict an energy cutoff for L_1-$L_{2,3}M_{4,5}$ transitions at $Z \cong 40$, while the cutoff for L_1-L_3M_5 transitions predicted from Dirac-Hartree-Slater calculations is at $Z \cong 50$; the latter prediction has been confirmed by experiment.[25]

A comparison is made in Fig. 7 of L_1-$L_{2,3}M_{4,5}$ Coster-Kronig rates computed with relativistic and nonrelativistic wave functions, the latter with relativistic and nonrela-

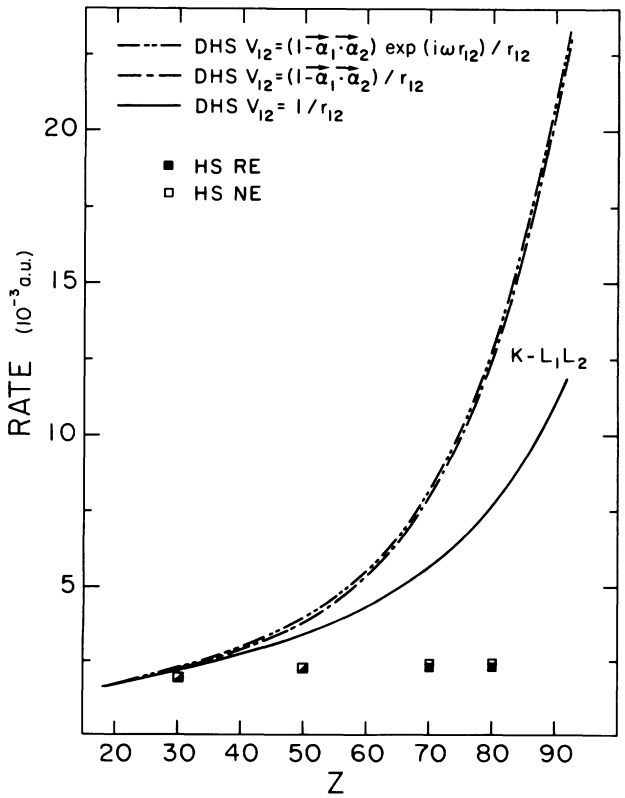

FIG. 9. Theoretical K-L_1L_2 Auger rates (in 10^{-3} a.u.), as functions of atomic number Z. Notation is as in Fig. 8.

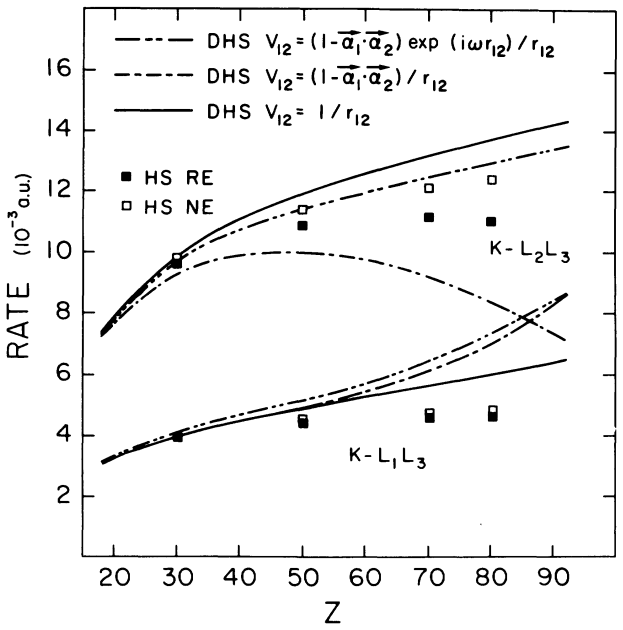

FIG. 10. Theoretical K-L_1L_3 and K-L_2L_3 Auger rates (in 10^{-3} a.u.), as functions of atomic number Z. Notation is the same as in Fig. 8.

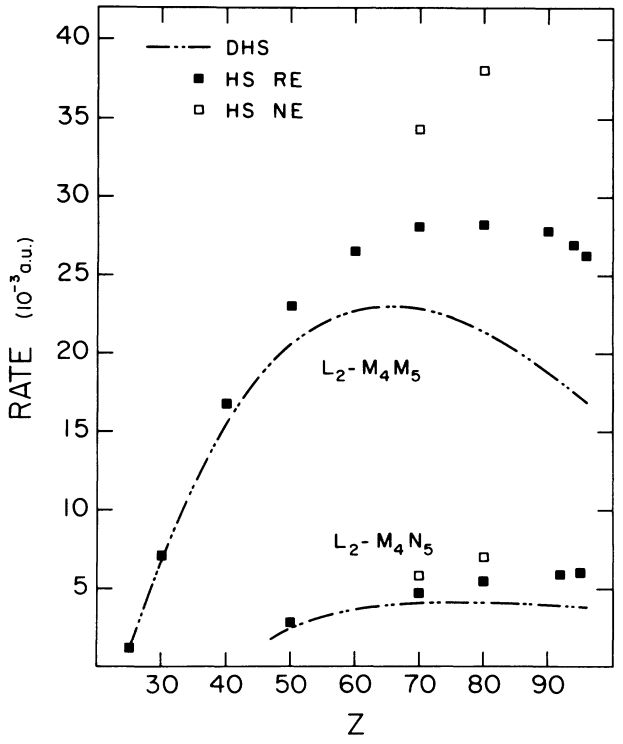

FIG. 11. Calculated L_2-M_4M_5 and L_2-M_4N_5 Auger transition probabilities (in 10^{-3} a.u.), as functions of atomic number Z. Results of relativistic computations with Dirac-Hartree-Slater wave functions and the complete two-electron operator of Eq. (27c) are compared with nonrelativistic rates calculated from Hartree-Slater wave functions with relativistic transition energies (solid squares) and nonrelativistic transition energies (open squares).

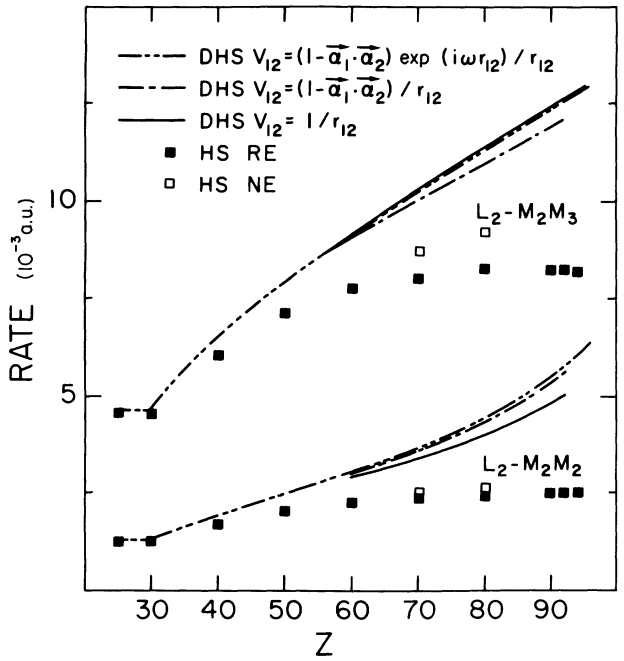

FIG. 12. Theoretical L_2-$M_2M_{2,3}$ Auger transition rates (in 10^{-3} a.u.), as functions of atomic number Z. Notation is the same as in Fig. 8.

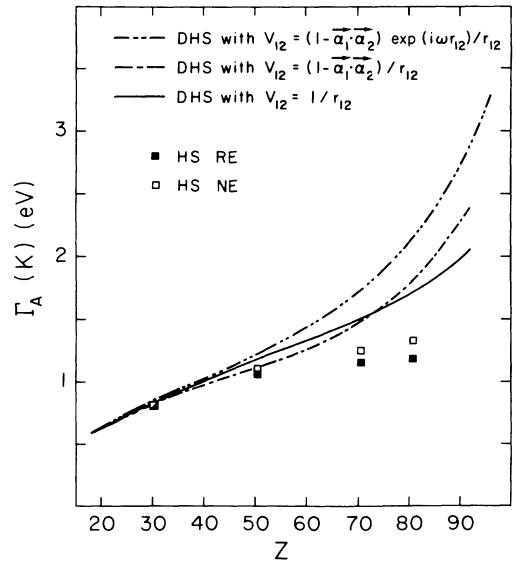

FIG. 14. Calculated total Auger widths (in eV) of [1s] (K-shell) vacancy states, as functions of atomic number Z. Notation is as in Fig. 8.

tivistic transition energies. This comparison clearly illustrates the fact that the effect of relativity on Coster-Kronig transitions is dominated by relativistic changes in the transition energies.

The effect of using different two-electron operators [Eqs. (27)] has been explored through calculations of K- and L-shell Auger matrix elements. Both Dirac-Hartree-Slater wave functions and nonrelativistic Hartree-Slater wave functions were employed, with both relativistic and nonrelativistic transition energies. The results, illustrated in Figs. 8—15, lead to the following observations.

(1) The energy effect on K-L_1L_1, K-L_1L_2, K-L_1L_3, and L_2-M_2M_2 transition rates is small because the relativistic energy shifts largely cancel out between initial and final states.

(2) For K-LL transitions, important effects usually arise from all factors: energy and wave-function changes, magnetic interaction, and retardation correction.

(3) The nonrelativistic K-L_1L_1 rates are greatly enhanced if we use relativistic wave functions, and increased further by the current-current interaction and by retardation. The K-L_3L_3 rates, on the other hand, are re-

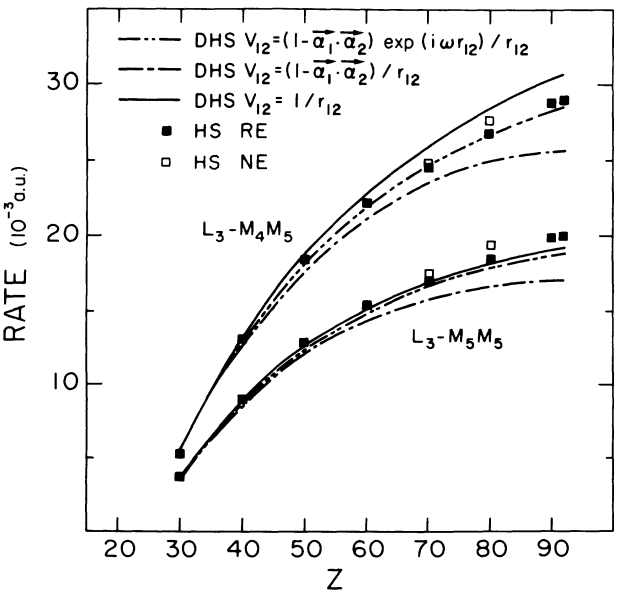

FIG. 13. Theoretical L_3-M_4M_5 and L_3-M_5M_5 Auger rates (in 10^{-3} a.u.), as functions of atomic number Z. See caption of Fig. 8 for explanation.

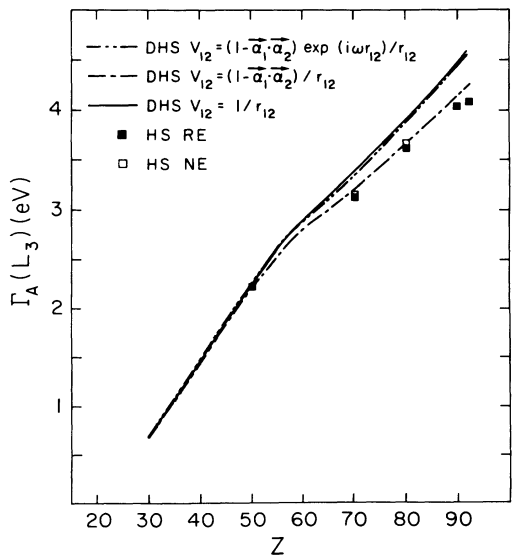

FIG. 15. Theoretical Auger widths (in eV) of [$2p_{3/2}$] (L_3-subshell) vacancy states, as functions of atomic number Z. Notation is as in Fig. 8.

duced by relativistic energy and wave functions, decreased further by the current-current interaction, but increased by the effect of retardation—to the extent that the net effect of relativity becomes quite small. A nearly complete cancellation is seen in the K-L_2L_3 rates, where the energy effect and magnetic interaction counteract the wave-function effect and retardation correction. By contrast, we note the huge effect that both the relativistic wave functions and the current-current interaction have on the K-L_1L_2 rates, which are enhanced by more than an order of magnitude in heavy elements.

(4) For the L-shell transitions, we again find the interplay of energy, wave-function, magnetic, and retardation effects. Here too, they can nearly cancel, as for the L_3-M_4M_5 rates (Fig. 13). Generally, for L-MM transitions, the relativistic energy changes and the orbital wave-function effect are more important than the magnetic interaction and the retardation correction. For L_2-$M_2M_{2,3}$, the relativistic effect is dominated by the change in wave functions. An example of a very pronounced effect of relativity is found in the L_2-M_4M_5 transitions (Fig. 11), for which energy, wave functions, and retardation reduce the Coulomb term, and the magnetic term is out of phase with the Coulomb term, so that it further reduces the rate.

(5) The exact effect of including relativity in the calculation of Auger rates cannot be predicted in general terms without going through the specific calculations. It depends on the relative strengths and phases of all factors involved (i.e., energy, wave-function, magnetic, and retardation effects).

(6) For total Auger level widths, which are sums of a large number of transition rates, the disparity of relativistic effects on individual rates tends to average out to some extent (Figs. 14 and 15). Nevertheless, for the K shell, a pronounced increase in the Auger widths is found, close to a factor of 3 at the high end of the Periodic Table.

Sample calculations with Dirac-Fock wave functions have not altered the conclusions reached here from work with Dirac-Hartree-Slater wave functions.

ACKNOWLEDGMENTS

We thank Hans Mark for his continued interest in this work. One of us (B.C.) wishes to express his appreciation for the hospitality of the Stanford Synchrotron Radiation Laboratory and the Physics Department of Stanford University. This work was supported in part by the U.S. Air Force Office of Scientific Research through Contract No. F49620-83-K-0020.

*Permanent address: Department of Physics and Chemical Physics Institute, University of Oregon, Eugene, Oregon 97403.

[1]A. I. Akhiezer and V. B. Berestetskii, *Quantum Electrodynamics* (Interscience, New York, 1965).

[2]V. B. Berestetskii, E. M. Lifshitz, and L. P. Pitaevskii, *Quantum Electrodynamics* (Pergamon, Oxford, 1982).

[3]A. F. Starace, Phys. Rev. A 3, 1242 (1971); 8, 1141 (1973); L. Armstrong, Jr., W. R. Fielder, and Dong L. Lin, *ibid.* 14, 1114 (1976); L. Armstrong, Jr., in *Structure and Collisions of Ions and Atoms,* edited by I. A. Sellin (Springer, Berlin, 1978), Chap. 3; M. Vajed-Samii, D. Ton-That, and L. Armstrong, Jr., Phys. Rev. A 23, 3034 (1981).

[4]J. H. Scofield, Phys. Rev. 179, 9 (1969); At. Data Nucl. Data Tables 14, 121 (1974).

[5]H. R. Rosner and C. P. Bhalla, Z. Phys. 231, 347 (1970).

[6]C. P. Bhalla, J. Phys. B 3, 916 (1970); Phys. Rev. A 2, 2575 (1970).

[7]J. H. Scofield, Phys. Rev. A 9, 1041 (1974).

[8]R. J. S. Crossley, Adv. Atom. Mol. Phys. 5, 237 (1969).

[9]W. N. Asaad, Proc. R. Soc. London, Ser. A 249, 555 (1959).

[10]M. A. Listengarten, Izv. Akad. Nauk SSSR, Ser. Fiz. 25, 803 (1961) [Bull. Acad. Sci. USSR, Phys. Ser. 25, 803 (1961)]; 26, 182 (1962) [26, 182 (1962)].

[11]C. P. Bhalla, J. Phys. B 3, L9 (1970); 3, 916 (1970); Phys. Rev. A 2, 722 (1970); C. P. Bhalla and D. J. Ramsdale, J. Phys. B 3, L14 (1970).

[12]M. H. Chen, B. Crasemann, and H. Mark, Phys. Rev. A 21, 436 (1980).

[13]M. H. Chen, B. Crasemann, and H. Mark, Phys. Rev. A 24, 177 (1981); M. H. Chen, E. Laiman, B. Crasemann, M. Aoyagi, and H. Mark, *ibid.* 19, 2253 (1979).

[14]M. H. Chen, B. Crasemann, and H. Mark, Phys. Rev. A 21, 449 (1980).

[15]M. H. Chen, B. Crasemann, K. R. Karim, and H. Mark, Phys. Rev. A 24, 1845 (1981).

[16]I. P. Grant, J. Phys. B 7, 1458 (1974).

[17]K.-N. Huang, J. Phys B 11, 787 (1978).

[18]J. B. Mann and W. R. Johnson, Phys. Rev. A 4, 41 (1971).

[19]M. H. Mittleman, in the Proceedings of the Workshop on Foundations of the Relativistic Theory of Atomic Structure, Argonne National Laboratory Report No. ANL-80-128 (unpublished).

[20]G. E. Brown and D. G. Ravenhall, Proc. R. Soc. London, Ser. A 208, 552 (1951).

[21]I. P. Grant, B. J. McKenzie, P. H. Norrington, D. F. Mayers, and N. C. Pyper, Comput. Phys. Commun. 21, 207 (1980).

[22]K.-N. Huang, M. Aoyagi, M. H. Chen, B. Crasemann, and H. Mark, At. Data Nucl. Data Tables 18, 243 (1976).

[23]W. Bambynek, B. Crasemann, R. W. Fink, H.-U. Freund, H. Mark, C. D. Swift, R. E. Price, and P. V. Rao, Rev. Mod. Phys. 44, 716 (1972).

[24]M. H. Chen, B. Crasemann, K.-N. Huang, M. Aoyagi, and H. Mark, At. Data Nucl. Data Tables 19, 97 (1977).

[25]B. L. Doyle and S. M. Shafroth, Phys. Rev. A 19, 1433 (1979).